

## EDGE ARTICLE

View Article Online  
View Journal | View IssueCite this: *Chem. Sci.*, 2021, 12, 10538

All publication charges for this article have been paid for by the Royal Society of Chemistry

## Pyridylphosphonium salts as alternatives to cyanopyridines in radical–radical coupling reactions†

Jacob W. Greenwood, Benjamin T. Boyle and Andrew McNally\*

Radical couplings of cyanopyridine radical anions represent a valuable technology for functionalizing pyridines, which are prevalent throughout pharmaceuticals, agrochemicals, and materials. Installing the cyano group, which facilitates the necessary radical anion formation and stabilization, is challenging and limits the use of this chemistry to simple cyanopyridines. We discovered that pyridylphosphonium salts, installed directly and regioselectively from C–H precursors, are useful alternatives to cyanopyridines in radical–radical coupling reactions, expanding the scope of this reaction manifold to complex pyridines. Methods for both alkylation and amination of pyridines mediated by photoredox catalysis are described. Additionally, we demonstrate late-stage functionalization of pharmaceuticals, highlighting an advantage of pyridylphosphonium salts over cyanopyridines.

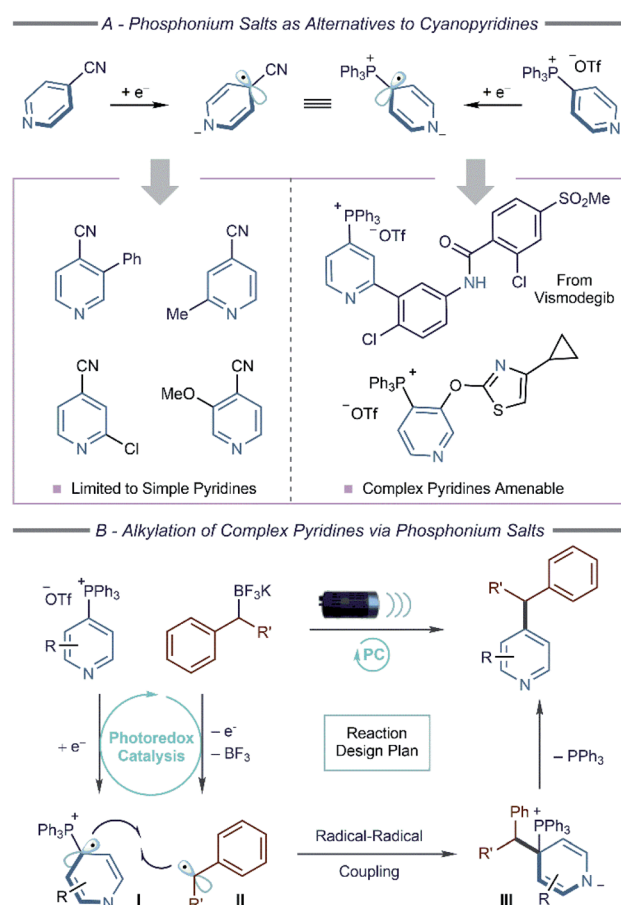
Received 27th April 2021  
Accepted 28th June 2021

DOI: 10.1039/d1sc02324a

rsc.li/chemical-science

Modern photoredox catalysis and electrochemistry have enabled new synthetic methods that proceed *via* open-shell intermediates.<sup>1</sup> Under this regime, pyridine functionalization strategies have been developed where 4-cyanopyridines undergo single-electron reduction to form dearomatized radical species that couple with other stabilized radicals (Scheme 1A).<sup>2</sup> The cyano group is critical for efficient reactivity *via* pyridyl radical anions; alternatives such as 4-halopyridines more readily undergo elimination to pyridyl radicals after single-electron reduction resulting in a distinct set of coupling processes.<sup>3</sup> We aimed to show that pyridylphosphonium salts could replicate the reactivity of cyanopyridines and allow a broader set of inputs into dearomatized pyridyl radical coupling reactions.<sup>4</sup>

Cyanopyridines have facilitated pyridine alkylation, allylation, and alkenylation reactions providing access to valuable building blocks for medicinal and agrochemical programs.<sup>5</sup> The cyano group is essential for these methods, but a problem arises when applying this chemistry to complex pyridines, such as those found in pharmaceutical and agrochemical candidates. These structures are often devoid of pre-installed functional groups, and it is often challenging to install a cyano group from C–H precursors regioselectively.<sup>6</sup> We envisioned pyridylphosphonium salts, regioselectively constructed from the C–H bonds of a diverse set of pyridines, could serve as alternatives to cyanopyridines.<sup>7</sup> Herein, we report couplings between alkyl BF<sub>3</sub>K salts and preliminary studies of carboxylic acids and amines with pyridylphosphonium salts, including late-stage



Scheme 1 Expansion of radical coupling reactions to complex pyridines.

Department of Chemistry, Colorado State University, Fort Collins, Colorado 80523, USA. E-mail: andy.mcnelly@colostate.edu

† Electronic supplementary information (ESI) available. See DOI: 10.1039/d1sc02324a

functionalization of complex pyridine-containing pharmaceuticals using this strategy.

Recently, we reported a radical coupling reaction between a boryl-stabilized cyanopyridyl radical and a boryl-stabilized pyridylphosphonium radical.<sup>7a</sup> The intermediate radicals arose *via* an unusual inner-sphere process that would be difficult to extend to other coupling reactions. A significant advance would be to show that pyridylphosphonium salts could function more generally as radical anion precursors and mimic the reactivity of cyano-pyridines. In particular, showing their viability in photoredox and electrochemical processes would translate to numerous synthetic transformations. To demonstrate this principle, we envisioned a redox-neutral alkylation reaction (Scheme 1B) *via* a radical coupling between radical zwitterion **I**, formed through single-electron reduction of a pyridylphosphonium salt ( $E_{\text{red}}^{\text{red}} = -1.51$  V vs. SCE) and benzyl radical **II**, resulting from single-electron oxidation of a  $\text{BF}_3\text{K}$  salt ( $E^{\text{red}} = +1.10$  V vs. SCE for a primary benzylic salt).<sup>8</sup> Loss of triphenylphosphine from dearomatized intermediate (**III**) would furnish the alkylated pyridine product. Notably, the

redox events could invert, where the photocatalyst oxidizes the  $\text{BF}_3\text{K}$  salt first and reduces the pyridylphosphonium salt second, broadening the scope of amenable photocatalysts.

We began our investigation by examining a series of photocatalysts for the coupling reaction of phosphonium salt **1a**, formed with complete regioselectivity for the 4-position from 2-phenylpyridine, and benzylic  $\text{BF}_3\text{K}$  salt **2a** under irradiation from a 455 nm Kessil light (Table 1A and available redox potentials and triplet state energies of photocatalysts shown in Table 1B). We discovered that both  $\text{Ir}(\text{ppy})_3$  and  $[\text{Ir}(\text{dF}(\text{CF}_3)\text{ppy})_2(\text{dtbbpy})]\text{PF}_6$  catalyze the transformation despite markedly different redox properties (entries 1 and 2), suggesting that the order of redox events in Scheme 1B are potentially interchangeable.<sup>1b</sup> The Adachi-type photocatalyst 3DPAFIPN improved the yield to 77% with a further increase to 82% after increasing the reaction concentration (entries 3 and 4). Adding 2,6-lutidine, previously shown as an effective additive for photoredox cross-coupling reactions of  $\text{BF}_3\text{K}$  salts by the Molander group,<sup>9</sup> had no impact on the yield of 2-phenylpyridine salt **1a** (entry 5) and the  $[\text{Ir}(\text{ppy})_2(\text{dtbbpy})]\text{PF}_6$  catalyst was marginally

Table 1 Optimization of pyridine alkylation, photocatalyst data and effect of  $\text{BF}_3\cdot\text{OEt}_2$  as an additive<sup>a</sup>

A – Reaction Optimization					
Entry	Salt	Photocatalyst (2 mol%)	Additive (3 equiv)	Concentration	% 3a <sup>b</sup>
1	<b>1a</b>	$\text{Ir}(\text{ppy})_3$	none	0.1 M	60
2	<b>1a</b>	$[\text{Ir}(\text{dF}(\text{CF}_3)\text{ppy})_2(\text{dtbbpy})]\text{PF}_6$	none	0.1 M	66
3	<b>1a</b>	3DPAFIPN	none	0.1 M	77
4	<b>1a</b>	3DPAFIPN	none	0.3 M	82
5	<b>1a</b>	3DPAFIPN	2,6-lutidine	0.3 M	82 (74) <sup>c</sup> (74) <sup>d</sup>
6	<b>1a</b>	$[\text{Ir}(\text{ppy})_2(\text{dtbbpy})]\text{PF}_6$	2,6-lutidine	0.3 M	74
7	<b>1b</b>	3DPAFIPN	none	0.3 M	20 <sup>e</sup>
8	<b>1b</b>	3DPAFIPN	2,6-lutidine	0.3 M	60 <sup>f</sup> (42) <sup>c</sup>
9	<b>1a</b>	none	2,6-lutidine	0.3 M	trace
10 <sup>g</sup>	<b>1a</b>	none	2,6-lutidine	0.3 M	66
11	<b>1a</b>	$[\text{Mes-Acr}]\text{BF}_4$	2,6-lutidine	0.3 M	41

B – Photocatalyst Redox Properties, and Triplet State Energies <sup>h</sup>					
Photocatalyst	$\text{Ir}(\text{ppy})_3$	$[\text{Ir}(\text{dF}(\text{CF}_3)\text{ppy})_2(\text{dtbbpy})]\text{PF}_6$	$[\text{Ir}(\text{ppy})_2(\text{dtbbpy})]\text{PF}_6$		
$E_{1/2}(\text{PC}^+/\text{PC}^*)$	-1.73 V	-0.89 V	-0.96 V		
$E_{1/2}(\text{PC}^+/\text{PC}^-)$	+0.31 V	+1.21 V	+0.66 V		
$E_{1/2}(\text{PC}^+/\text{PC})$	+0.77 V	+1.69 V	+1.21 V		
$E_{1/2}(\text{PC}/\text{PC}^-)$	-2.19 V	-1.37 V	-1.57 V		
$T_1$	58.1	61.8	49.2		
$E_{0,0}(\text{kcal/mol})$	58.1	61.8	49.2		

C – $\text{BF}_3$ Additive Enables a Previously Ineffective Photocatalyst			
Photocatalyst	3DPAFIPN	$[\text{Mes-Acr}]\text{BF}_4$	$[\text{Ru}(\text{bpy})_3]\text{PF}_6$
$E_{1/2}(\text{PC}^+/\text{PC}^*)$	-1.38 V		-0.81 V
$E_{1/2}(\text{PC}^+/\text{PC}^-)$	+1.09 V	+2.18 V	+0.77 V
$E_{1/2}(\text{PC}^+/\text{PC})$	+1.30 V		+1.29 V
$E_{1/2}(\text{PC}/\text{PC}^-)$	-1.59 V	-0.49 V	-1.33 V
$T_1$	61.8	44.7	49.0
$E_{0,0}(\text{kcal/mol})$	61.8	44.7	49.0

Results		
	% <b>1a</b>	% <b>3a</b>
Without $\text{BF}_3\cdot\text{OEt}_2$	98 <sup>b</sup>	trace
With $\text{BF}_3\cdot\text{OEt}_2$	51 <sup>b</sup>	47 <sup>b</sup>

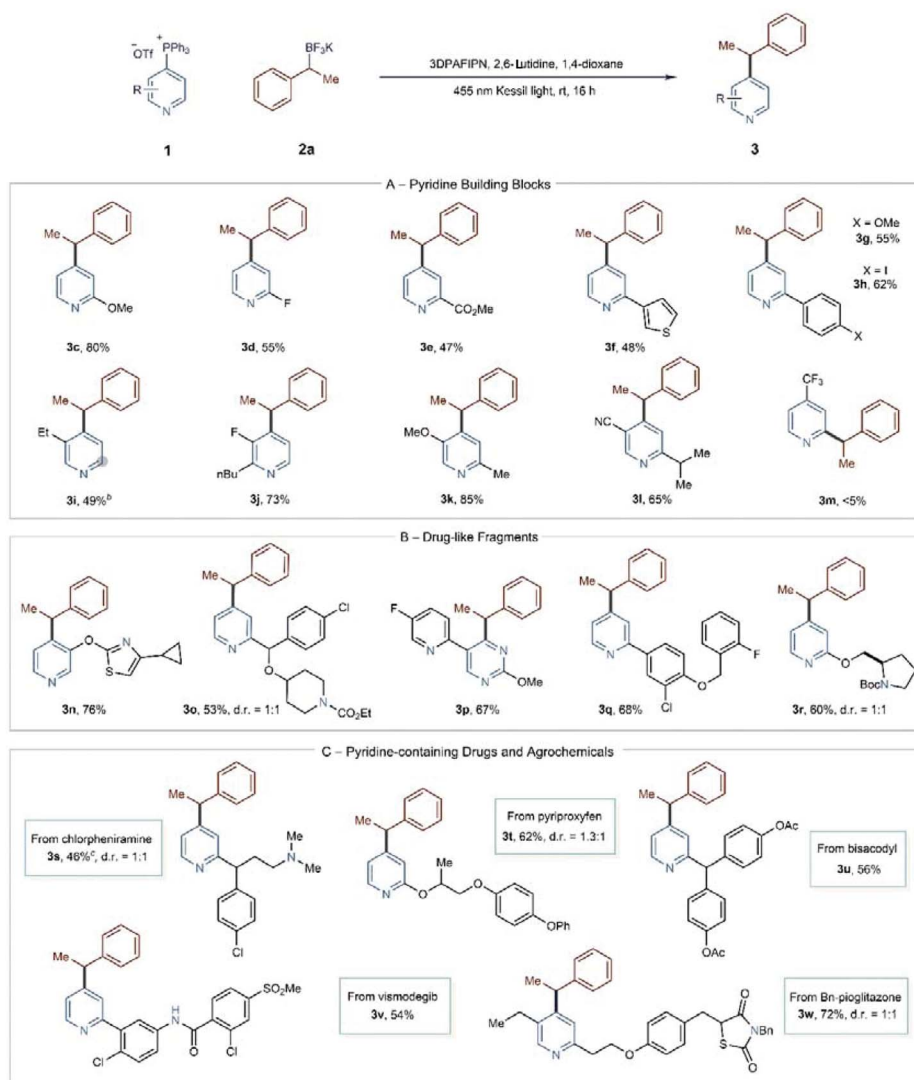
<sup>a</sup> Conditions: **1a** (1.0 equiv.), **2a** (2.0 equiv.), photocatalyst (2 mol%), additive (3.0 equiv.), rt. <sup>b</sup> Yields determined by <sup>1</sup>H NMR analysis using 1,3,5-trimethoxybenzene as internal standard. <sup>c</sup> Isolated yield on 0.50 mmol scale. <sup>d</sup> Isolated yield on 2.00 mmol scale. <sup>e</sup> **3**: **1** 4- vs. 2-regioisomeric ratio determined from the crude <sup>1</sup>H NMR. <sup>f</sup> **3**: **1** 4- vs. 2-regioisomeric ratio determined from the crude <sup>1</sup>H NMR. <sup>g</sup> Used 365 nm LEDs instead of 455 nm Kessil light for 89 h. <sup>h</sup> All redox potentials reported vs. SCE and all values compiled from previous literature reports.<sup>1</sup> <sup>i</sup> Counterion omitted in structure for simplicity.

less efficient under the same conditions (entry 6). We observed that 2,6-lutidine did substantially improve the yield when isomeric 3-Ph salt **1b** was employed (entries 7 and 8); without 2,6-lutidine, the crude  $^1\text{H}$  NMR indicates significant amounts of decomposition occurred, including 3-phenylpyridine, and the 4- vs. 2-position product ratio was 3 : 1. This outcome suggests that protidephosphination and non-selective Minisci-type pathways can occur under these conditions. With 2,6-lutidine, the crude reaction pathway is cleaner, and the 4- vs. 2-position ratio improved to 8 : 1. At this point, we have not established the role of 2,6-lutidine, although it is conceivable that it reacts with  $\text{BF}_3$  produced as the reaction progresses. In 2-substituted systems, steric hindrance around the pyridine N-atom of the salt would deter  $\text{BF}_3$ -coordination, whereas, in 3-substituted systems, such as salt **1b**, coordination is more likely and may

have a deleterious effect on the reaction (*vide infra*). Given the structural variation of pyridines that we anticipated applying to this process and how those structures could impact boron speciation during the reaction, we elected to use 2,6-lutidine as an additive in all subsequent reactions.<sup>10</sup>

We conducted a series of further experiments to explore the effect of light and photocatalyst type on the reaction (Table 1, entries 9–11). Irradiating the reaction at 455 nm without photocatalyst resulted in traces of **3a**, but we did observe 66% yield of the product when we used a 365 nm light (entries 8 and 9). No evidence of an electron donor–acceptor (EDA) complex was observable by UV-Vis spectroscopy, and we propose that the reaction starts by an overlap of the tails of the LEDs emission with the absorption of **1a** at 345 nm (see ESI†).<sup>11</sup> Furthermore, a photocatalyst with a redox potential window misaligned with

Table 2 Scope of heterocyclic phosphonium salt coupling partners<sup>a</sup>



<sup>a</sup> Isolated yields of single regioisomers. Conditions: **1** (1.0 equiv.), **2a** (2.0 equiv.), 3DPAFIPN (2 mol%), 2,6-lutidine (3.0 equiv.), 1,4-dioxane (0.3 M), rt. <sup>b</sup> 11 : 1 crude regioisomeric ratio. Isolated as a single regioisomer. Grey circle denotes the site of alkylation for the minor regioisomer. <sup>c</sup> With 1 equiv. TFOH.



the redox events in Scheme 1B, [Mes-Acr]BF<sub>4</sub>, is also competent (entry 11). An energy transfer mechanism was considered based on entry 9, but the low triplet state energies for [Mes-Acr]BF<sub>4</sub> make this pathway unlikely (Table 1B). However, this result suggests that other factors could influence the reaction mechanism. The results in Table 1C show that pyridine N-activation can play a significant role in some instances. Using Ru(bpy)<sub>3</sub> and 455 nm irradiation resulted in trace products but adding 1 equivalent of BF<sub>3</sub>·OEt<sub>2</sub> formed **3a** in 47% yield. Here, we hypothesize that **1a** reacts with BF<sub>3</sub> to enable single-electron reduction, and radical zwitterions of type **IV** are intermediates in the reaction. At this stage of our investigations, we conclude that radical zwitterions **I** and **IV** are likely present to varying extents depending on the photocatalyst and reaction conditions employed. Using optimal catalyst 3DPAFIPN and adding 2,6-lutidine to the reaction may favor **I** over **IV** and potentially indicate that **I** is more reactive in the C–C bond-forming step. Stern–Volmer quenching of 3DPAFIPN by pyridylphosphonium salt **1a** occurs ( $K_{SV} = 14.9 \text{ M}^{-1}$  and  $K_q = 3.55 \times 10^9 \text{ L mol}^{-1} \text{ s}^{-1}$ ), indicating that type **I** intermediates are accessible under the reaction conditions without BF<sub>3</sub>.<sup>12–14</sup>

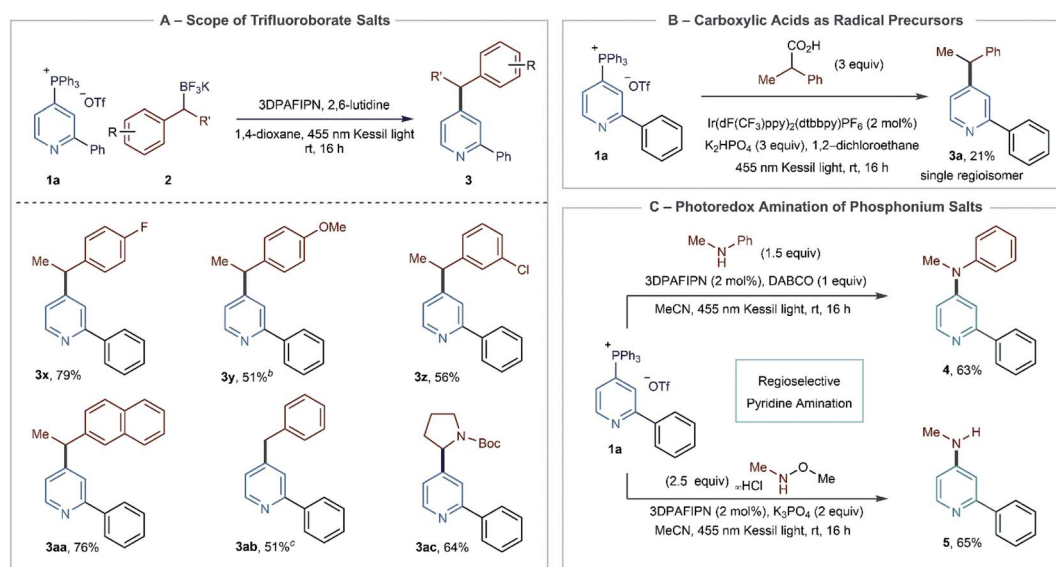
Employing the optimized conditions, we investigated the scope of pyridylphosphonium salts in this coupling process (Table 2). Starting with building block-type pyridines, 2-substituted pyridines with electron-withdrawing and electron-donating groups couple effectively (**3c–3e**). Aryl and heteroaryl groups are also compatible at the 2-position (**3f** & **3g**), and we did not observe any undesired reactivity of the carbon–iodine bond in **3h**. An 11 : 1 regioisomeric mixture of compounds formed when a 3-ethyl substituent was present (**3i**), but single isomers formed from 2,3- and 2,5-disubstituted pyridines (**3j–3l**). At present, 2-substituted pyridylphosphonium salts are not successful coupling partners; as a representative example, when we attempted to synthesize **3m**, we observed significant decomposition of the starting material

and only minor amounts (<5%) of the desired compound among other unidentified products.

Next, we converted a series of drug-like fragments and pharmaceuticals into phosphonium salts in this alkylation reaction. These examples represent the most significant advantage of this chemistry as installing a cyano group would be challenging from the C–H bond and limits the ability to make analog compounds. In addition, these structures contain multiple reactive sites and functional groups that could interfere with the coupling process. Nevertheless, we synthesized benzylated fragments **3n–3r** without difficulty. Notably, other heterocycles are compatible, such as thiazoles and protected piperidines and pyrrolidines. The pyridine–pyrimidine biaryl **3p** is particularly interesting as the phosphonium salt formed site-selectively on the pyrimidine ring, and the photoredox coupling proceeded in good yield on this heterocycle. Lastly, we demonstrated coupling with four FDA-approved pharmaceuticals and an agrochemical that illustrates functional group tolerance for protonated tertiary amines, amides, aryl halides, benzyl ethers, and sulfones (**3s–3w**). These examples validate this tactic for late-stage functionalization of complex pyridines.

Scheme 2A shows the scope of the BF<sub>3</sub>K salts in the photoredox alkylation reaction. Secondary benzylic salts with electron-withdrawing and electron-donating groups are suitable coupling partners (**3x–3z**). In the case of **3y**, we added a 1.2 : 1 mixture of benzylic and homobenzylic BF<sub>3</sub>K salts but only observed the benzylated product, presumably because the primary isomer is more difficult to oxidize. Secondary naphthyl and primary benzylic BF<sub>3</sub>K salts are proficient, resulting in **3aa** and **3ab**. The reaction also tolerates  $\alpha$ -amino BF<sub>3</sub>K salts as evidenced by heterobenzylic amine derivative **3ac**. At this stage, non-stabilized radicals were not successful in this process.

Finally, we investigated whether pyridylphosphonium salts are competent with other radical precursors. In Scheme 2B, we



**Scheme 2** Scope of radical coupling partners. <sup>a</sup>Isolated yields of single regioisomers. Conditions: **1a** (1.0 equiv.), **2** (2.0 equiv.), 3DPAFIPN (2 mol%), 2,6-lutidine (3.0 equiv.), 1,4-dioxane (0.3 M), rt. <sup>b</sup>BF<sub>3</sub>K starting material is 1.2 : 1 mixture of regioisomers (benzylic : primary). <sup>c</sup>>20 : 1 regioisomeric ratio and 5.7 : 1 mono : bis alkylated product in crude <sup>1</sup>H NMR spectrum. Isolated as single monoalkylated regioisomer.



obtained a preliminary result (unoptimized) of coupling with a carboxylic acid. These abundant compounds would improve the scope of radical coupling partners, and further studies are currently underway in our laboratory. In addition, Wu recently reported a method for photoredox catalyzed amination using cyanopyridines as coupling partners, and we attempted to replicate this transformation using pyridylphosphonium salts (Scheme 2C).<sup>15</sup> Applying salt **1a** to the reaction protocol with *N*-methyl aniline resulted in diaryl amine **4**.<sup>16</sup> Similarly, using *N,O*-dimethylhydroxylamine as a coupling partner, followed by *in situ* cleavage of the N–O bond, formed aniline **5** in reasonable yield. Consistent with the results in Table 2, we expect that this reaction will be compatible with more complex pyridine phosphonium salts and further suggests that phosphonium ions can serve as surrogates for cyanopyridines in other radical anion coupling reactions.

## Conclusions

In conclusion, we report that pyridylphosphonium salts behave as alternatives to cyanopyridines to extend the utility of radical-radical coupling reactions to more complex substrates. We showed that two distinct reactions, pyridine alkylation, and amination, can proceed *via* phosphonium-stabilized radical intermediates. Our lab is currently investigating the capacity of pyridylphosphonium salts to participate in other open-shell reactions, as well as the mechanisms described in this study.

## Data availability

All experimental procedures and data related to this study can be found in the ESI.

## Author contributions

AMC and JWG conceptualized the work. JWG and BTB performed the experiments in this project. AMC and JWG prepared the manuscript.

## Conflicts of interest

There are no conflicts to declare.

## Acknowledgements

The National Science Foundation supported this work under Grant No. (1753087). We also thank the Sloan Foundation, Amgen, and Eli Lilly for generous gifts that partially supported this work. We gratefully acknowledge the Shores and Miyake groups at CSU for their expertise and generous use of their equipment.

## Notes and references

- (a) J. Twilton, C. Le, P. Zhang, M. H. Shaw, R. W. Evans and D. W. C. MacMillan, *Nat. Rev. Chem.*, 2017, **1**, 0052; (b) C. K. Prier, D. A. Rankic and D. W. C. MacMillan, *Chem. Rev.*, 2013, **113**, 5322–5363; (c) J. M. R. Narayanam and C. R. J. Stephenson, *Chem. Soc. Rev.*, 2011, **40**, 102–113; (d) N. A. Romero and D. A. Nicewicz, *Chem. Rev.*, 2016, **116**, 10075–10166; (e) F. Strieth-Kalthoff, M. J. James, M. Teders, L. Pitzer and F. Glorius, *Chem. Soc. Rev.*, 2018, **47**, 7190–7202; (f) E. J. Horn, B. R. Rosen and P. S. Baran, *ACS Cent. Sci.*, 2016, **2**, 302–308.
- For selected examples, see: (a) A. McNally, C. K. Prier and D. W. C. MacMillan, *Science*, 2011, **334**, 1114–1116; (b) T. Hoshikawa and M. Inoue, *Chem. Sci.*, 2013, **4**, 3118; (c) Z. Zuo and D. W. C. MacMillan, *J. Am. Chem. Soc.*, 2014, **136**, 5257–5260; (d) J. D. Cuthbertson and D. W. C. MacMillan, *Nature*, 2015, **519**, 74–77; (e) F. Lima, M. A. Kabeshov, D. N. Tran, C. Battilocchio, J. Sedelmeier, G. Sedelmeier, B. Schenkel and S. V. Ley, *Angew. Chem., Int. Ed.*, 2016, **55**, 14085–14089; (f) S. Zhu, J. Qin, F. Wang, H. Li and L. Chu, *Nat. Commun.*, 2019, **10**, 749; (g) M. C. Nicastrì, D. Lehnher, Y. Lam, D. A. DiRocco and T. Rovis, *J. Am. Chem. Soc.*, 2020, **142**, 987–998; (h) Y. Ma, X. Yao, L. Zhang, P. Ni, R. Cheng and J. Ye, *Angew. Chem., Int. Ed.*, 2019, **58**, 16548–16552; (i) D. Lehnher, Y. Lam, M. C. Nicastrì, J. Liu, J. A. Newman, E. L. Regalado, D. A. DiRocco and T. Rovis, *J. Am. Chem. Soc.*, 2020, **142**, 468–478; (j) A. Yu. Vorob'ev, *Chem. Heterocycl. Compd.*, 2019, **55**, 90–92.
- In azoles, halides can facilitate homolytic aromatic substitution pathways, see: (a) C. K. Prier and D. W. C. MacMillan, *Chem. Sci.*, 2014, **5**, 4173–4178; (b) A. Singh, A. Arora and J. D. Weaver, *Org. Lett.*, 2013, **15**, 5390–5393.
- (a) R. A. Aycock, H. Wang and N. T. Jui, *Chem. Sci.*, 2017, **8**, 3121–3125; (b) C. P. Seath, D. B. Vogt, Z. Xu, A. J. Boyington and N. T. Jui, *J. Am. Chem. Soc.*, 2018, **140**, 15525–15534; (c) A. J. Boyington, C. P. Seath, A. M. Zearfoss, Z. Xu and N. T. Jui, *J. Am. Chem. Soc.*, 2019, **141**, 4147–4153; (d) C. P. Seath and N. T. Jui, *Synlett*, 2019, **30**, 1607–1614; (e) A. Singh, J. J. Kubik and J. D. Weaver, *Chem. Sci.*, 2015, **6**, 7206–7212; (f) S. Senaweera and J. D. Weaver, *J. Am. Chem. Soc.*, 2016, **138**, 2520–2523.
- (a) M. Baumann and I. R. Baxendale, *Beilstein J. Org. Chem.*, 2013, **9**, 2265–2319; (b) E. Vitaku, D. T. Smith and J. T. Njardarson, *J. Med. Chem.*, 2014, **57**, 10257–10274; (c) T. Eicher, S. Hauptmann and A. Speicher, *The Chemistry of Heterocycles: Structure, Reactions, Syntheses, and Applications*, Wiley-VCH, Weinheim, 3rd edn, 2012.
- (a) X. Yu, J. Tang, X. Jin, Y. Yamamoto and M. Bao, *Asian J. Org. Chem.*, 2018, **7**, 550–553; (b) D. Zhao, P. Xu and T. Ritter, *Chem*, 2019, **5**, 97–107; (c) B. L. Elbert, A. J. M. Farley, T. W. Gorman, T. C. Johnson, C. Genicot, B. Lallemand, P. Pasau, J. Flasz, J. L. Castro, M. MacCoss, R. S. Paton, C. J. Schofield, M. D. Smith, M. C. Willis and D. J. Dixon, *Chem.–Eur. J.*, 2017, **23**, 14733–14737.
- (a) J. L. Koniarczyk, J. W. Greenwood, J. V. Alegre-Requena, R. S. Paton and A. McNally, *Angew. Chem., Int. Ed.*, 2019, **58**, 14882–14886; (b) J. L. Koniarczyk, D. Hesk, A. Overgard, I. W. Davies and A. McNally, *J. Am. Chem. Soc.*, 2018, **140**, 1990–1993; (c) X. Zhang and A. McNally, *ACS Catal.*, 2019,



- 9, 4862–4866; (d) M. C. Hilton, R. D. Dolewski and A. McNally, *J. Am. Chem. Soc.*, 2016, **138**, 13806–13809; (e) C. B. Kelly and R. Padilla-Salinas, *Chem. Sci.*, 2020, **11**, 10047–10060.
- 8 J. K. Matsui, D. N. Primer and G. A. Molander, *Chem. Sci.*, 2017, **8**, 3512–3522.
- 9 (a) J. C. Tellis, D. N. Primer and G. A. Molander, *Science*, 2014, **345**, 433–436; (b) J. C. Tellis, J. Amani and G. A. Molander, *Org. Lett.*, 2016, **18**, 2994–2997; (c) J. K. Matsui, Á. Gutiérrez-Bonet, M. Rotella, R. Alam, O. Gutierrez and G. A. Molander, *Angew. Chem., Int. Ed.*, 2018, **57**, 15847–15851.
- 10 Using benzyltrifluoroborate, the  $^1\text{H}$  NMR yield of product **3aa** decreased from 50% to 29% when 2,6-lutidine was omitted.
- 11 G. H. Lovett, S. Chen, X.-S. Xue, K. N. Houk and D. W. C. MacMillan, *J. Am. Chem. Soc.*, 2019, **141**, 20031–20036.
- 12 We thank an anonymous reviewer for suggesting that intermediates **I** are more reactive than **IV** to explain the role of 2,6-lutidine.
- 13 L. Cardinale, M. O. Konev and A. Jacobivon Wangelin, *Chem.–Eur. J.*, 2020, **26**, 8239–8243.
- 14 Despite the similarities in photophysical properties between photocatalysts  $\text{Ru}(\text{bpy})_3(\text{PF}_6)_2$  and  $\text{Ir}(\text{ppy})_2(\text{dtbbpy})\text{PF}_6$ , the iridium photocatalyst works well in the absence of  $\text{BF}_3$  additive while  $\text{Ru}(\text{bpy})_3(\text{PF}_6)_2$  requires it. The reason for this is not yet understood and studies to explain this observation are ongoing.
- 15 C. Zhou, T. Lei, X.-Z. Wei, C. Ye, Z. Liu, B. Chen, C.-H. Tung and L.-Z. Wu, *J. Am. Chem. Soc.*, 2020, **142**, 16805–16813.
- 16 Excluding the 3DPAFIPN resulted in traces (<1%) of **4**. Control reactions also show that DABCO does not displace the phosphonium ion in **1a** to form an ammonium salt.

